Pulsar Observations at Urumqi Observatory
— Present and Future

Na Wang[1],   R. N. Manchester [2],   Jin Zhang[1],   Xinji Wu[3]   &   Ali Esamudin[1,3]

(1 *National Astronomical Observatories, CAS, Urumqi* 830011)
(2 *Australia Telescope National Facility, CSIRO, P.O. Box 76, Epping, NSW 1710, Australia*)
(3 *Department of Astronomy, Peking University, Beijing* 100871)

ABSTRACT   We present the status and results of pulsar observations at Urumqi Observatory. Observations commenced with a pulsar timing system at the 25-m Urumqi Nanshan telescope in mid-1999; these were the first regular and high-quality pulsar observations in China. The center frequency of this system is 1540 MHz, and de-dispersion is provided by a $2 \times 128 \times 2.5$ MHz filterbank/digitiser system. Observations over more than one year have resulted in updated positions and period parameters for 74 pulsars. Comparing with earlier observations we showed that long-term period and period-derivative fluctuations may be dominated by unseen glitches. Taking advantage of the available telescope time, we are also monitoring the variation of pulsar scintillation dynamic spectra for a few strong pulsars. Scintillation parameters are measured and their variations are under study. We are planning to built a new system at a lower frequency so that frequency-dependent pulsar properties can be investigated.

1   Introduction

The first pulsar observation was made in late 1967, and since then much progress has been made in understanding their properties. Pulsars are also used as probes to investigate the gravitational wave background and the interstellar medium. However because of the lack of a suitably instrumented radio telescope, China did not contribute much to the pulsar observations in the past few decades, but this has now changed. This paper introduces pulsar observations and results obtained with a 25-m radio telescope operated by Urumqi Observatory. This telescope is located near the geographic center of Asia with longitude 87 deg, latitude +43 deg and altitude 2080m. The telescope was initially constructed as a VLBI station; a back-end system for pulsar studies in the 18-cm band was developed in mid-1999. The pulsar project at Urumqi is a collaboration between Urumqi Observatory, Peking University, Hong Kong University, the Australia Telescope National Facility and Jodrell Bank Observatory.

De-dispersion is provided by a $2 \times 128 \times 2.5$ MHz filterbank/digitizer system. The receiver was a room-temperature, dual-polarization one, but a new more sensitive cryogenic receiver was commissioned in July 2002. However, the results discussed in this paper were obtained between 2000 January and 2002 June with the room-temperature receiver. This receiver allowed us to observe pulsars with a flux density greater than about 4 mJy, so we monitored 74 detectable pulsars to study their timing properties. One reason for us to do this is that the catalog for these stronger pulsars had not been updated for many years, some of them even more than 30 years. Based on the timing system we started regular scintillation observations for five pulsars from January 2001. We report the results of pulsar

timing observations in Sections 2 and 3 and scintillation observation in Sections 4. In the last section we discuss the future scope of pulsar programs at Urumqi Observatory.

2   Timing Observations

2.1   Updated Parameters and the Unseen Glitch Model

Frequent observations of 74 pulsars resulted in updated periods and period derivatives, as discussed in detail by Wang et al. (2001). The accuracy of period measurements is generally better than 0.1 ns, and typical residuals are a few hundred microseconds. By comparing the new measurements with the best previous observation, we obtained the variations in periods and period derivatives, i.e., ΔP and $\Delta \dot{P}$ respectively over long time intervals, up to 30 years. The changes in periods are in the range of 10^{-9} to 10^{-8} s, excluding few pulsars which have glitched or those with errors in ΔP larger than 20 ns. We found a correlation between the period and period-derivative changes which is shown in Figure 1. The period and period-derivative changes tend to have the same sign and to be correlated in amplitude. This correlation is improved when more recent data are included, compared to that shown in Wang et al. (2001). Random period noise would not produce such correlated changes in P and $\dot{P}$, however relaxation from unseen glitches may do so.
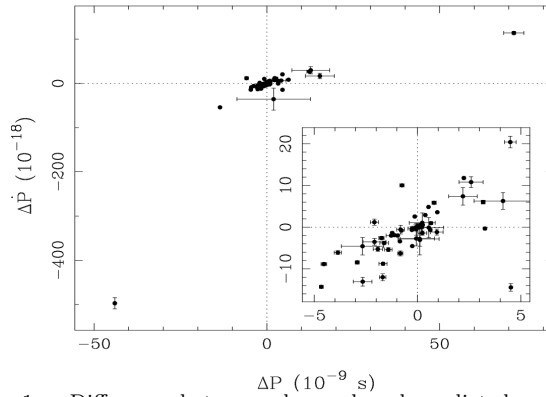
Fig. 1   Difference between observed and predicted period derivative $\Delta\dot{P}$, plotted against difference in period, ΔP. The inset is an expanded version of the central region.

In most cases, the pulse frequency after a glitch can be described by an exponential decay function:

$$\nu(t) = \nu_0(t) + \Delta\nu_g[1 - Q(1 - \exp(-t/\tau_d)] + \Delta\dot{\nu}_p t\,, \tag{1}$$

where $\nu_0(t)$ is the value of ν extrapolated from before the glitch, $\Delta\nu_g$ is the total frequency change at the time of the glitch, Q is the fractional part of $\Delta\nu_g$ which decays away exponentially, τ_d is the decay time constant and $\Delta\dot{\nu}_p$ is the permanent change in $\dot{\nu}$ at the time of the glitch. The increment in frequency derivative is given by:

$$\Delta\dot{\nu}(t) = \frac{-Q\Delta\nu_g}{\tau_d}\exp(-t/\tau_d) + \Delta\dot{\nu}_p\,. \tag{2}$$

We assume that the present results or the catalog values are contaminated by an unseen glitch, and use the above glitch functions to extrapolate back the period and period derivative

changes caused by the glitch relaxation process. In the analysis, the glitch epoch is arbitrarily taken as 400 days before the present observation, the relative change is $\Delta\nu/\nu = 10^{-6}$, and time constant $\tau_d = 100$ d. For post-glitch relaxation we considered the situations of no decay, part decay and total decay of the period jump, and a permanent increase, decrease or no change in the period derivative at the time of the glitch. This model agrees well with the observational results, in which the amplitude and sign in ΔP and $\Delta\dot{P}$ are correlated (see Figure 2). The model also works for the very special Crab pulsar glitches, in which both ΔP and $\Delta\dot{P}_p$ are positive after the glitch. This agreement suggests that long-term period and period derivative changes are dominated by decay from unseen glitches.
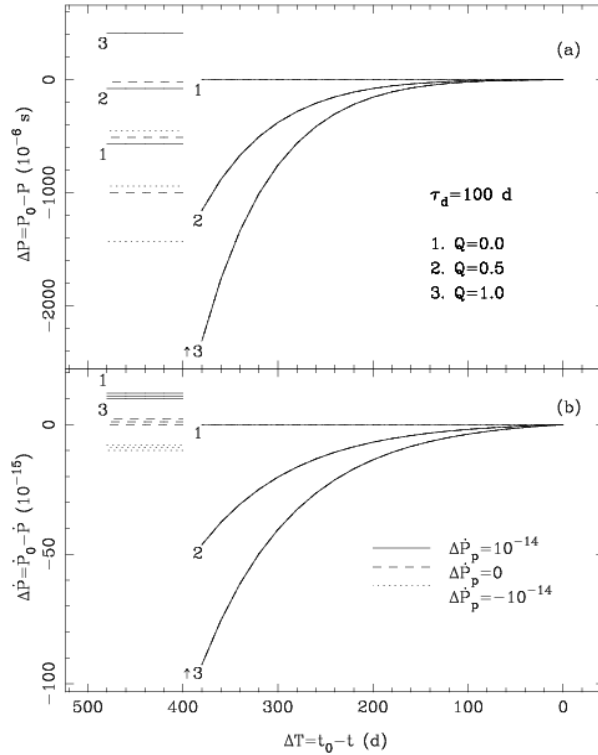
Fig. 2   A model for the increments in pulse period and period derivative due to a glitch occurring 400 days before the current time t_0. A glitch magnitude $\Delta\nu_g = 10^{-6}$ and a post-glitch decay time of 100 days are assumed. Changes for three different decay parameters Q and three different permanent changes in period derivative $\Delta\dot{P}_p$ are plotted. The groups of three lines of one type are for different values of Q and the solid, dashed and dotted lines represent different values of $\Delta\dot{P}_p$. The post-glitch values are functions of Q and independent of $\Delta\dot{P}_p$, so they overlap for different $\Delta\dot{P}_p$.

2.2 Glitches

Frequent observations at Urumqi have revealed five glitches up to June 2002. Table 1 lists the glitch pulsars and glitch epochs in the first two columns, and the glitch sizes are given in the third column. Columns four and five list the jump in frequency derivative at the glitch, $\Delta\dot{\nu}$, and the permanent jump in frequency derivative, $\Delta\dot{\nu}_p$, respectively. The decaying part in frequency jump, $\Delta\nu_d$, is given in column six, and the decay time constant τ_d and fractional decay Q are given in the last two columns.

Figure 3 shows the variations in pulse frequency and frequency derivative in the Crab

pulsar over the MJD interval 51600 to 52420, covering the two most recent glitches. Both glitches have a permanent jump in $\Delta\dot\nu_{\rm p}$. Figure 3 doesn't show the detail of the glitch decay process for the second glitch; this could be due to the rapid post-glitch decay in this pulsar (Wong, Backer & Lyne, 2001) combined with the large gap between the observations. PSR B1737−30 is a well-known young pulsar which glitches about every 300 days (Shemar & Lyne, 1996). In our observation, this pulsar was quite stable for about 700 days, and then suddenly glitched three times in about 120 days, with two small glitches followed by a larger one. Figure 4 shows the phase residuals over these glitches - a slope change indicates a jump in pulse period. PSR J1835−1106 is a young pulsar which has no previously reported glitch.

Table 1 Glitches detected by Urumqi 25m radio telescope

PSR	Epoch (MJD)	$\Delta\nu/\nu$	$\Delta\dot\nu$ (10^{-9})	$\Delta\dot\nu_{\rm p}$ $(10^{-15}{\rm s}^{-2})$	$\Delta\nu_{\rm d}$ $(10^{-6}{\rm s}^{-1})$	$\tau_{\rm d}$ (d)	Q
B0531+21	51740.8	23(15)		−37(17)	0.5(4)	4	0.8(8)
	52082(2)	10.5(1)		−62(2)			
B1737−30	52234(2)	5.3(9)					
	52268(2)	13.2(9)					
	52347.4	152.8(5)	−1.32(14)				
1835−1106	52224(2)	23(5)			0.020(6)	100	0.21(6)
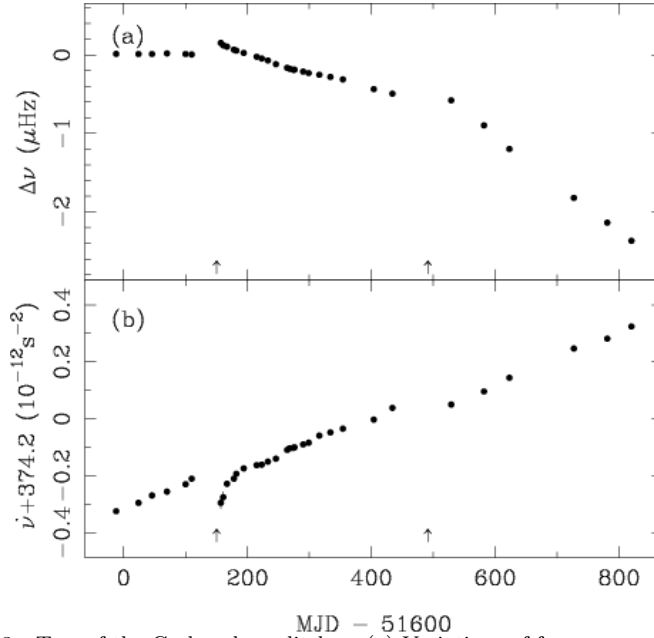
Fig. 3   Two of the Crab pulsar glitches. (a) Variations of frequency residual $\Delta\nu$ relative to the pre-glitch solution, and (b) the variations of $\dot\nu$. The glitch parameters are given in Table 1.

3 Proper Motion Measurements

The accuracy of position measurements is typically a few milliarcseconds with two and a half years observation. By comparing them with best previous measurements, we obtained the position differences and hence the proper motions given in Table 2. Column five gives
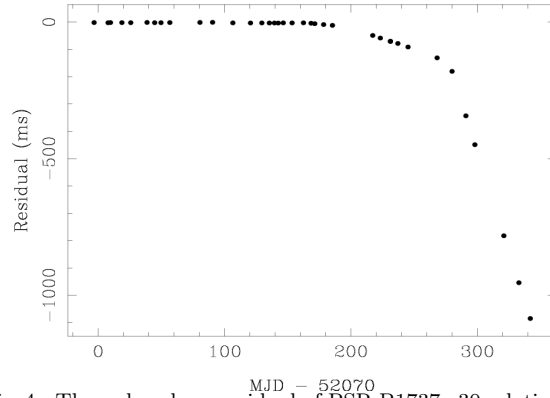
Fig. 4   The pulse phase residual of PSR B1737−30 relative to
the pre-glitch solution, the slope change indicate a glitch.

transverse velocities based on distances from the new distance model NE2001 (Cordes & Lazio 2002) given in column four. Since we have only two and half years data, these results may be contaminated by long-term timing noise although the measurements seem significant. How reliable they are remains to be checked from further observations.

Table 2   Proper motion and pulsar velocity

PSR Name		Proper Motion	Distance	V_{pm}
(J2000)	(B1950)	(mas/y)	(kpc)	(km/s)
0332+5434	0329+54	12(4)	0.972	55(20)
0358+5413	0355+54	16(5)	1.447	110(40)
0454+5543	0450+55	73(8)	0.659	228(25)
0630−2834	0628−28	58(7)	1.444	400(50)
0738−4042	0736−40	57(4)	0.567	157(5)
1136+1551	1133+16	385(7)	0.333	608(11)
1239+2453	1237+25	116(7)	0.799	441(27)
1935+1616	1933+16	20(1)	5.556	531(25)
1948+3540	1946+35	18(2)	5.721	480(60)
2257+5909	2255+58	27(7)	4.495	570(160)
2313+4253	2310+42	33(8)	1.243	200(50)

4   Scintillation Observations

Regular scintillation observations for five pulsars started in January 2001 with one observation about every 10 days on average. These pulsars are PSRs B0329+54, B0823+26, B1929+10, B2020+28 and B2021+51. Each observation lasts between two and six hours, mostly depending on the typical correlation timescale for diffractive interstellar scintillation (DISS), which is proportional to $D^{-3/2}$, where D is the pulsar distance. For example, for PSR B0329+54, each observation is about three hours, but more nearby pulsars such as PSR B1929+10 are observed for six hours mostly. The 18 months of data have shown major variations in the scintillation dynamic spectra for each of these pulsars. The left side of Figure 5 shows such changes for PSR B0329+54. We see the scintle size changes with time, which indicates variations in the DISS time scale τ_d and the decorrelatin frequency scale $\Delta\nu_d$. Systematic drifts of the pattern are observed frequently for PSR B0329+54, showing the effects of refractive scintillation (RISS). The right side of Figure 5 is the secondary spectrum – the two-dimensional Fourier transform of the scintillation dynamic spectrum.

The extra power at higher frequencies shown in observations at MJDs 52027.4, 52078.3, 52202.5 are due to the finer fringes in their dynamic spectra.

These spectra have been corrected for the effects of interference in the observation band. The interference may be narrow-band and long-term or broad-band and short-term. The narrow band interference is most serious at around 1480 MHz, 1550 MHz and 1620 MHz, normally across few frequency channels. The broad-band interference occured only occasionally and typically lasts one or two sub-intergration times, which in our observation is four minutes. To provide a clean data set for further analysis, we use a linear interpolation across the bad data.
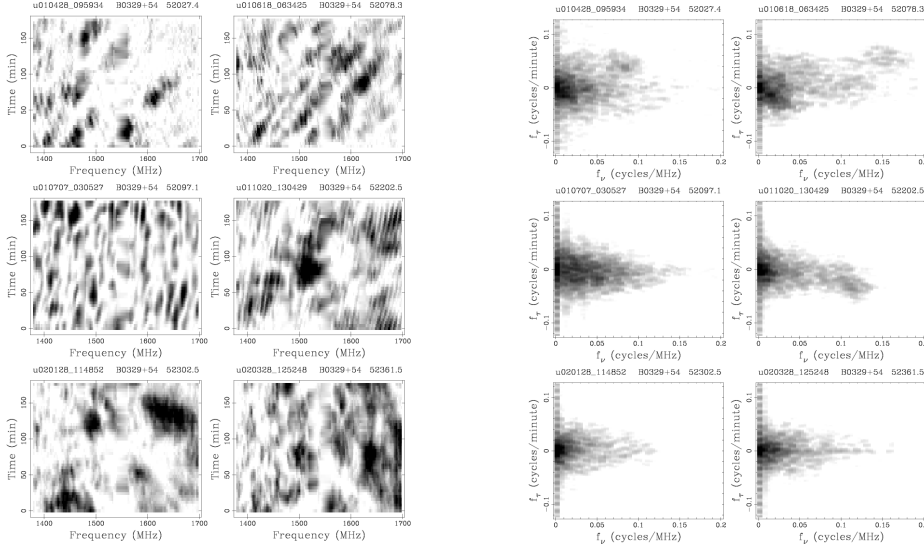
Fig. 5 Scintillation dynamic spectra (left) and secondary spectra (right) for PSR B0329+54.

The parameters of diffractive scintillation are obtained from the two-dimensional auto-correlation function (ACF) of the dynamic spectrum (Cordes, 1986). We applied a two-dimensional Gaussian fit to ACF, from which the scintillation time scale τ_{d}, decorrelation frequency scale $\Delta\nu_{\mathrm{d}}$ and the tilt of the ellipse hence the slope of the dynamic spectra are derived (cf. Stinebring, Faison & McKinnon, 1996). τ_{d} is defined as the half-width at $1/e$ of the maximum of the Gaussian in time, and $\Delta\nu_{\mathrm{d}}$ to be the half-width at half-maximum of the Gaussian in frequency. The top two panels in Figure 6 show the variation of τ_{d} and $\Delta\nu_{\mathrm{d}}$. The third panel is a derived parameter, the pulsar scintillation velocity V, which is calculated based on a density fluctuation spectral slope of 4.0 in the scattering screen (Gupta, Rickett & Lyne, 1994). Panel four is the slope of the dynamic spectrum which indicates the drifting rate of the pattern. Panel five is the mean flux density of each observation. We checked the consistency of DISS parameters with the dynamic spectra, and they are in good agreement. The variation of adjacent points are also correlated, so the temporal changes of these parameters in Figure 6 are realistic. The observed variations of scintillation parameters indicates that the feature of the scattering disk change significantly with time. The fluctuation of the flux density also shows that due to the scintillation modulation, care has to be taken with the measurement of this quantity. Many observations over a long time span are necessary to obtain a reliable result, especially for closer pulsars at higher frequencies.
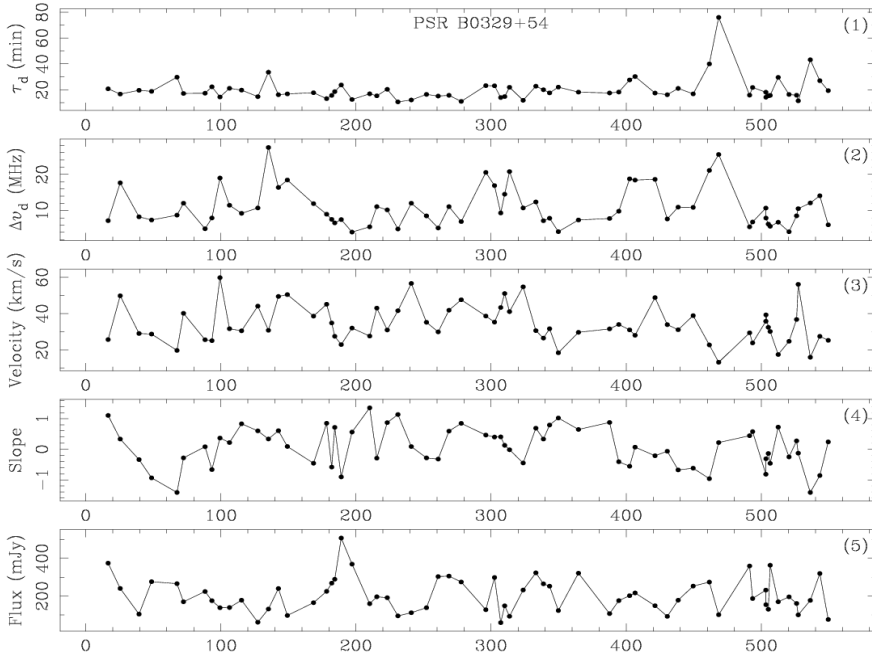
Fig. 6   Time variation of scintillation parameters and derived parameters for PSR B0329+54.

5 Profiles and Flux Density Variation

The grand mean pulse profiles of each pulsar are formed by adding data corresponding to good timing points over the data span. Calibration was done by choosing several distant pulsars which have good flux density measurements in the catalogue. Based on the digitiser counts, the timing analysis program TREDUCE (developed at Swinburne University of Technology and ATNF) can give a number which is proportional to the mean flux density. A scale factor is then computed to convert the TREDUCE number into a flux density. Some of the system effects such as systematic changes of the receiver sensitivity are removed before this. We consider the modulation index m or r.m.s. variation/mean here. Figure 7 shows a plot of modulation index versus the logarithm of dispersion measure (DM); the dashed line is proportional to $DM^{-1/3}$. The pulsars generally form two groups. The first consists of the nearby pulsars where the DISS is the main effect and the modulation is weak with $m < 1$. The second group is the larger DM pulsars, where DISS effect is weaker and RISS is stronger. The observed relationship of $m \propto DM^{-1/3}$ is expected from RISS theory, so the observed flux density fluctuations are dominated by propagation effects rather than intrinsic changes in the pulse emission.

6 Prospect of Future Work

A new cryogenic receiver has been designed and built at ATNF for Urumqi Observatory. This state-of-the-art receiver was installed in July 2002 and it greatly improves the system performance. It gives the system temperature of about 22 K, allowing us to detect pulsars as weak as 1 mJy, which means a great increase in the number of detectable pulsars. With the larger sample of pulsars, our main interests will remain in pulsar timing, scintillation
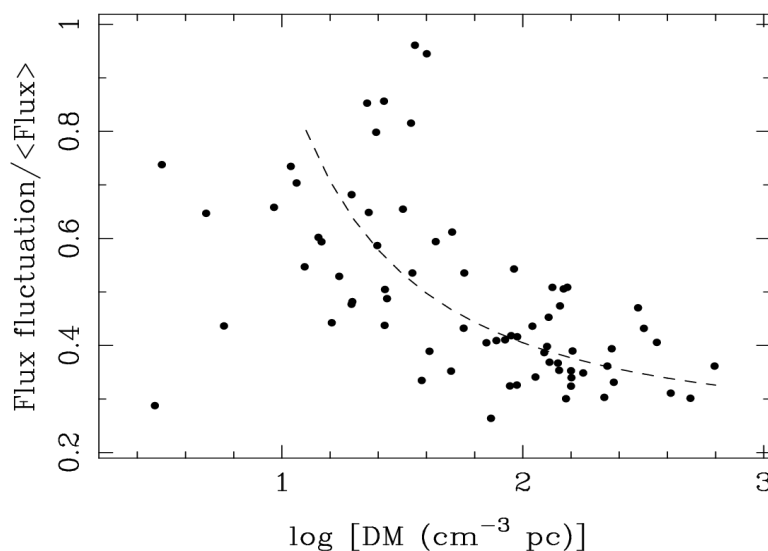
Fig. 7   Relative flux density fluctuation versus dispersion measure. The dashed line is proportional to $DM^{-1/3}$.

and studies of the pulse emission mechanism.

To broaden the pulsar study area and complement the present 18-cm observations, a digital de-dispersing system at a lower frequency such as 660 MHz is planned. This system will be based on the Jodrell Bank Observatory COBRA (Coherent Online Baseband Receiver for Astronomy) system. The baseband system with coherent dedispersion can give high time and frequency resolution, enhancing the profile resolution and timing precision at these lower frequencies. It also provides polarisation information allowing studies of both individual pulses and mean pulse profiles. We plan to construct a new more sensitive receiver at 660 MHz for this system.

We are also planning to develop a pulsar searching system at the telescope. The availability of telescope time and the wide beam allows us to search wide areas. Investigation of the associations of unidentified gamma-ray sources with pulsars was the initial motivation for this project.

References

Cordes J.M., ApJ, 1986, 311, 183
Cordes J.M., Lazio, astro-ph/0207156 2002
Gupta Y., Rickett B.J., Lyne A.G., MNRAS, 1994, 269, 1035
Shemar S.L., Lyne A.G., MNRAS, 1996, 282, 677
Stinebring D.R., Faison M.D., McKinnon M., ApJ., 1996, 460, 460
Wang N., Manchester R.N., Zhang J., et al., MNRAS, 2001, 328, 855
Wong T., Backer D.C., Lyne A.G., ApJ, 2001, 548, 447